Thermal Characteristics of an Unsteady Hybrid Nano-Casson Fluid Passing Through a Stretching Thin-Film with Mass Transition

Nur Ilyana Kamis[1], Noraihan Afiqah Rawi[1], Lim Yeou Jiann[1], Sharidan Shafie[1,*], Mohd Rijal Ilias[2]

[1] Department of Mathematical Sciences, Faculty of Science, Universiti Teknologi Malaysia, 81310 UTM Johor Bahru, Johor, Malaysia
[2] Faculty of Computer and Mathematical Sciences, Universiti Teknologi MARA, 40450 Shah Alam, Selangor, Malaysia

ABSTRACT

In current communication, the thin-film flow of Casson hybrid nanofluid consists of copper and alumina nanoparticles that dissolved in carboxymethyl cellulose (CMC) plus water over an unsteadystretching porous sheet is elucidated. Using suitable similarity variables, the resultant partial governing equations are turned into a set of nonlinear ordinary differential equations. The Keller box approach is then used to solve the transformed equations. The unknown thin-film thickness constant is determined by using the homotopy analysis approach. The thermal and velocity distributions, as well as the Nusselt number and skin friction of the fluid, are discussed for different values of relevant parameters such as thin-film thickness, nanoparticles volume fraction, and mass transition parameter. The distributions of temperature and velocity decrease when the thin-film thickness is increased. The velocity distribution is decreased by the Casson, nanoparticles volume fraction, and mass transition (injection) parameter. The temperature is enhanced by the nanoparticle's volume fraction and the Casson parameter, however, has an opposite tendency with the mass transition (injection) parameter. For the physical quantities, the skin friction has a negative function with all the parameters. The mass transition (injection) parameter increases the Nusselt number. The outcomes of the present study are useful for example in producing the smart contact lens that has been used in the biomedical field.

1. Introduction

Recently, technological developments have encouraged researchers to conduct various studies to meet the needs of consumers. One of the investigations is about the analysis of heat transfer as it can create mechanical merchandise or apparatuses that function admirably for the manufacturing process and industrial engineering these days. The presence of nanoparticles in a fluid influences thermal transfer properties. Choi [1] defined the nanofluid as a merger of solid nanoparticles in a base liquid. Nanofluid is observed to provide high heat transfer rates in a thermal energy system. Khan *et al.,* [2] investigated the flow of a boundary layer nanofluid past a constant stretching sheet.

The concerned nanofluid model consists of thermophoresis as well as Brownian motion effects, which are also called Buongiorno's model. Jahad *et al.,* [3] described an unsteady heat transfer in a nanofluid with suction and injection. A similar mathematical model to Khan *et al.,* [2] was utilized. The investigation revealed that in nanofluids, suction and injection parameters have a considerable impact on temperature and velocity profiles as well as physical quantities. However, most studies, including Yirga and Shankar [5,6], Hafidz *et al.,* [6,7], and Gangadhar *et al.,* [8,9], have investigated heat transfer of a nanofluid model, namely Tiwari and Das' [4] model. Using the Keller box approach, Yirga and Shankar [5] encountered the governing equations of MHD flow and heat transfer. The model of Tiwari and Das demonstrates the thermophysical properties of nanofluid including, density, specific heat capacity, dynamic viscosity, thermal, and electrical conductivity [5-7].

The heat transfer with nanoparticles in non-Newtonian Casson fluid past an unsteady stretched sheet was examined in a variety of situations due to its unique properties among non-Newtonian fluids [8-12]. The fluid was proposed by Casson [13] for producing the flow behavior of pigment-oil suspensions. According to Husannan *et al.,* [14], Casson is a form of viscoplastic fluid. The Casson fluid model is a shear-thinning liquid with a zero viscosity at an infinite rate of shear, as well as yield stress below which no flow occurs. Furthermore, Casson's shear stress rate relation explains the properties of a wide variety of polymers across a wide range of shear rates [15]. Jamshed *et al.,* [8] claimed that the speed of molecules in Casson fluid decay as the Casson and volume fraction parameters increase by dealing with the Keller box method. The effect of injection declines the velocity profile of Casson nanofluid [9]. Rawi *et al.,* [11] showed that the Keller box technique solves the fluid issue efficiently in the presence of copper (Cu) in carboxymethyl cellulose solution (CMC) over the stretching sheet. The presence of nanoparticles volume fraction and Casson parameter upsurge the thermal distribution but opposite trends for the fluid motion.

The mixture of different nanoparticles in a fluid which is termed "hybrid nanofluids" grabbed the response of the industry and engineering. This is because of its extensive technical, industrial, and scientific applications like transportation, microfluidics, medical manufacturing, etc. Outstanding heat transmission qualities have been achieved by the ideal combination of several nanoparticle features. [16]. According to the study of Devi and Devi [17] and Waini *et al.,* [18], the heat transfer rate of hybrid nanofluid, Cu and Al_2O_3 (aluminum oxide) is greater than nanofluid, Cu. The numerical simulation for the different nanoparticles namely Al_2O_3, TiO_2 (titanium dioxide), Cu and CuO (copper oxide) dispersed in CMC plus water was reported by Maleki *et al.,* [19]. They found that the concentration of nanoparticles in CMC-water as a base fluid enhances the Nusselt number of the heat transfer fluid. Venkateswarlu and Satya [20] discovered that the heat transfer of a hybrid nanofluid of $Cu\text{-}Al_2O_3$ which is measured in terms of the Nusselt number was lower than the single nanofluid. In the presence of thermal radiation, Sakkaravarthi *et al.,* [21] scrutinized the hybrid Ta (tantalum) and Co (cobalt) in the blood (Casson fluid) across a porous curved stretching sheet. They detected that the thermal radiation and magnetic parameters raise the temperature profile.

Thin-film flows are common in engineering, geophysics, biology, and other fields. The study of laminar thin-film flow over moving vertical, horizontal, or inclined flat plates is presently focused on the development of several experts since it has a huge potential to be used as a mechanical instrument in various designing applications. For example, coating, draining, biological, solar cells, and wetting involve thin-film fluid flow [23]. Wang [24] investigated the hydrodynamics of a thin liquid film for Newtonian fluid over a stretched sheet without taking thermal performance into account. Wang [24] was inspired by the research efforts of Sakiadis [25], Crane [26], and Carragher and Crane [27], who investigated the effect of heat transfer on the fluid flow when the sheet is stretched. Andersson *et al.,* [28] initiated an inquiry into the nature of Wang's [24] hydrodynamic

heat transfer problem Wang's [24] approach was expanded by Andersson *et al.,* [28], who incorporated the similarity transformation for the thermal equation. An ordinary differential equation for energy equation is obtained when applied the new similarity of the thermal field thin-film fluid. The behavior of the heat transfer in thin-film flow has a significant effect when the unsteadiness parameter is embedded in thin-film fluid flow at low Prandtl numbers. Wang [29] then extended the work done by Wang [24] to include the flow problem with heat transfer. To obtain the solution for the analyzed parameters, the homotopy analysis technique (HAM) was used by Wang [26]. Xu *et al.,* [30] expanded on Wang's [29] by taking into account the existence of nanoparticles in a thin-film fluid. This study considered the model provided by Tiwari and Das [4]. It was found that the usage of the nanoparticles in the thin-film liquid gives a more prominent effect on the temperature profile compared to the fluid speed. Numerous investigations on the flow of nanofluids that address the thin-film flow may be found in papers by Giri *et al.,* [31], Turkyilmazoglu [32], Pal *et al.,* [33] and Lu *et al.,* [34]. According to Sulochana and Aparna [22], the presence of hybrid nanoparticles, Al_2O_3-Cu in thin-film flow enhances the heat transfer rate compared to a single nanofluid.

Due to the broad applications in the engineering sector in the design of microfabrication, solar thin-film, and photovoltaic thin-film [35], the investigation of boundary layers flow of non-Newtonian embedded with the thin-film has received great research interest. Recently, several researchers investigated the Casson fluid in thin-film [36,37] and also nanofluid [38-41] past a stretching sheet with various effects and fluid models. Rehman *et al.,* [36] published a comparison of HAM as an analytical and bvp4c as a numerical output on Casson fluid with slip and uniform thickness, as well as suction and injection effects. The package BVPh2.0 with the help of MATHEMATICA was used to compute the solution for the HAM. Numerical and analytical methods have shown good agreement.

Coating of the thin-film is useful in the production of smart contact lenses in the optical industry. The current work is motivated by the preceding literature survey. The study of Wang [29], Xu *et al.,* [30], and Sulochana and Aparna [22] are extended for an unsteady thin-film Casson hybrid nanofluid flow with injection or mass transition effect past a stretching sheet. Furthermore, the predominant idea is pursued in light of the publications by Rawi *et al.,* [11] and Rehman *et al.,* [36]. The impact of hybrid nanoparticles, as hypothesized by Devi and Devi [17] and Sulochana and Aparna [22], is examined and visually displayed. The modified model by Tiwari and Das [4] for the hybrid nanofluid is employed. Therefore, the present study aims to investigate the Casson hybrid nanofluid flow in a thin-film under the influence of mass transition (injection) over an unsteady stretching sheet. The existence of the nanoparticles in the fluid can improve the change rate of heat and working fluid properties due to their special features [42]. The outputs of the present study are useful in producing an advanced transparent contact lens, such as coating a thin protective layer against harmful radiations in the lenses [43]. A similarity transformation approach is applied to determine the nonlinear ordinary differential equations (ODEs) from the nonlinear partial governing equations (PDEs). The nonlinear and dimensionless ODEs are then numerically solved using the Keller box technique, an implicit finite difference approach.

2. Mathematical Formulation

This work investigates Casson fluid flow in a thin liquid film of uniform thickness, $h(t)$ with a horizontal plane at the $x-$axis through a tiny slit. The $y-$axis is perpendicular to the $x-$axis, as illustrated in Figure 1 [29]. The fluid motion within the film is caused the elastic sheet being stretched. The sheet is stretching itself with the velocity $U_w = bx(1-\alpha t)^{-1}$ [29]. $b > 0$ and $\alpha > 0$ are the positive constants with dimension per time that emerge in the stretched rate. The elastic sheet,

which is anchored at the origin, is stretched by applying a force in the positive direction of x and $b(1 - \alpha t)^{-1}$ indicates the rate of effective stretching that grows as time passes because because $\alpha > 0$. Furthermore, at $y = 0$, the surface temperature, T_w in terms of slit temperature, T_0 and reference temperature, T_{ref}, may be described as $T_w = T_0 - T_{ref}\left(\frac{bx^2}{2v}\right)(1 - \alpha t)^{-\frac{3}{2}}$ [29]. Here, T_w is expected to vary with distance from the slit in this case. The temperature at the stretching sheet decreases in proportion to x^2 from the narrow slit's temperature, and the temperature decreases with the sheet lifting over time. Furthermore, the expression $\left(\frac{bx^2}{2v}\right)(1 - \alpha t)^{-\frac{3}{2}}$ may be defined as the local Reynold number that relies on the surface velocity, U_w. At the boundary conditions, the fluid flow in a thin-film is additionally embedded with the mass transition parameter, $V_w = \frac{(V_w)_0}{(1 - \alpha t)^{0.5}}$ [42] where $(V_w)_0$ refers to the initial velocity mass transition parameter. Furthermore, the Casson hybrid nanofluid is injected, $V_w < 0$ at the thin-film sheet. Incompressible Casson hybrid nanofluid governing equations may be rewritten as [22, 29, 36]
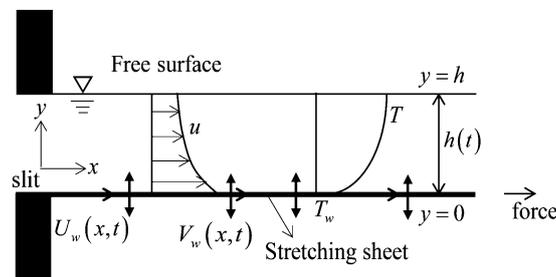
Fig. 1. Physical model

$$\frac{\partial u}{\partial x} + \frac{\partial v}{\partial y} = 0, \tag{1}$$

$$\rho_{hnf}\left[\frac{\partial u}{\partial t} + u\frac{\partial u}{\partial x} + v\frac{\partial u}{\partial y}\right] = \mu_{hnf}\left[1 + \frac{1}{\beta}\right]\frac{\partial^2 u}{\partial y^2}, \tag{2}$$

$$(\rho c_p)_{hnf}\left[\frac{\partial T}{\partial t} + u\frac{\partial T}{\partial x} + v\frac{\partial T}{\partial y}\right] = k_{hnf}\frac{\partial^2 T}{\partial y^2}, \tag{3}$$

where (u, v) denotes velocity segments along x and y axes. The Casson fluid parameter is $\beta = \frac{\mu_B\sqrt{2\pi_c}}{p_y}$ where μ_B represents the plastic dynamic viscosity, p_y is yield stress, and π_c is the critical value of this product based on the Casson model. Heat conduction, specific heat capacity, density, and effective dynamic viscosity of hybrid nanofluid are represented by $k_{hnf}, (C_p)_{hnf}, \rho_{hnf}, \mu_{hnf}$, respectively. T and t demonstrate the temperature and time. The boundary conditions for Eq. (1) to (3) are as follows, assuming that the planar fluid film's surface is smooth and free of surface waves [22,29,44]

$$y = 0 : u = U_w, v = V_w, T = T_w, \tag{4}$$

$$y = h : \frac{\partial u}{\partial y} = \frac{\partial T}{\partial y} = 0, v = \frac{dh}{dt}. \tag{5}$$

The top free surface of the liquid film at $y = h$ in contact with a passive gas is considered to be flat, and the effect of surface tension is assumed to be insignificant. Hybrid nanoparticles that consist of copper, Cu and aluminium oxide, Al_2O_3 are dissolved in the conventional heat transfer Casson fluid which incorporates carboxymethyl cellulose (CMC) and water as acknowledged by Ali *et al.,* [45-46]. Because the viscosity is based on shear stress, CMC plus water is one of the most prevalent kinds of time-independent non-Newtonian fluid. This fluid exhibits shear-thinning or pseudoplastic rheology. Table 1 displays the thermophysical properties of the nanoparticles together with base fluid, as reported by [22,46,48]

Table 1
Thermophysical properties of the fluids

Physical properties	CMC plus water (0.0-0.4%)	Cu	Al_2O_3
$C_p (Jkg^{-1}K^{-1})$	4179	385	765
$\rho (kgm^{-3})$	997.1	8933	3970
$k (Wm^{-1}K^{-1})$	0.613	400	40
Pr	6.2	-	-

Eq. (1) to (3) are PDEs when applied to boundary conditions (4) and (5). Using the similarity transformations shown below, these equations may be reduced to the simplest set of an ODE [29]

$$\psi = [vb(1 - \alpha t)^{-1}]^{\frac{1}{2}} x \xi f(\eta), \tag{6}$$

$$T = T_0 - T_{ref}\left(\frac{bx^2}{2v}\right)(1 - \alpha t)^{-\frac{3}{2}}\theta(\eta), \tag{7}$$

$$\eta = \left(\frac{b}{v}\right)^{\frac{1}{2}}(1 - \alpha t)^{-\frac{1}{2}}\xi^{-1}y, \tag{8}$$

where an indefinite constant, ξ denotes the dimensionless thickness of the film, η represents the similarity variable, and the stream function, $\psi(x, y, t)$ may be expressed as [29]

$$u = \frac{\partial\psi}{\partial y} = \frac{bx}{(1 - \alpha t)}f', \tag{9}$$

$$v = -\frac{\partial\psi}{\partial x} = -\left(\frac{vb}{1 - \alpha t}\right)^{\frac{1}{2}}\xi f, \tag{10}$$

which fulfills continuity Eq. (1) automatically. When $y = h(t)$ at $\eta = 1$, for the free surface, Eq. (8) provides [29]

$$\eta = \left(\frac{b}{v}\right)^{\frac{1}{2}}(1 - \alpha t)^{-\frac{1}{2}}h(t), \tag{11}$$

which gives

$$\frac{dh}{dt} = -\frac{1}{2}\alpha\xi\left(\frac{v}{b}\right)^{\frac{1}{2}}(1-\alpha t)^{-\frac{1}{2}}. \tag{12}$$

Now, by imposing Eq. (6) to (10), the following is obtained

$$\left(\frac{A_1}{A_2}\right)\left(1+\frac{1}{\beta}\right)f''' + \lambda\left[ff'' + f'^2 - S\left(f' + \frac{1}{2}\eta f''\right)\right] = 0, \tag{13}$$

$$\left(\frac{A_3}{A_4}\right)Pr^{-1}\theta'' + \lambda\left[-S\left(\frac{3}{2}\theta + \frac{1}{2}\eta\theta'\right) - 2f'\theta + f\theta'\right] = 0, \tag{14}$$

and the boundary conditions become

$$\eta = 0: \; f'(0) = 1, f(0) = w, \theta(0) = 1, \tag{15}$$

$$\eta = 1: \; f''(1) = 0, \theta'(1) = 0, f(1) = \frac{S}{2}, \tag{16}$$

where the prime signifies the difference with respect to η. Here, λ is the thin-film thickness, Pr demonstrates the Prandtl number, S denotes the dimensionless unsteadiness, w is the mass transition parameter, and $A_i(i = 1,2,3,4)$ are changes in the thermophysical characteristics of hybrid nanofluids that may be characterized as [17,48]

$$\lambda = \xi^2, S = \frac{\alpha}{b}, Pr = \frac{(\mu c_p)}{k}, w = -\frac{(V_w)_0}{\xi\sqrt{vb}}, \tag{17}$$

$$A_1 = \frac{1}{[1 - (\phi_1 + \phi_1)^{2.5}]},$$
$$A_2 = \left[(1-\phi_2)\phi_1\frac{\rho_{s_1}}{\rho_{bf}} + \phi_2\frac{\rho_{s_2}}{\rho_{bf}} + (1-\phi+\phi_1\phi_2)\right],$$
$$A_3 = \left[\frac{k_{s_2} + 2k_{nf} - 2\phi_2(k_{bf} - k_{s_2})}{k_{s_2} + 2k_{nf} + \phi_2(k_{bf} - k_{s_2})}\right]\left[\frac{k_{s_1} + 2k_{bf} - 2\phi_2(k_{bf} - k_{s_1})}{k_{s_1} + 2k_{bf} + \phi_2(k_{bf} - k_{s_1})}\right]$$

where

$$k_{nf} = \left[\frac{k_{s_1} + 2k_{bf} - 2\phi_2(k_{bf} - k_{s_1})}{k_{s_1} + 2k_{bf} + \phi_1(k_{bf} - k_{s_1})}\right]k_{bf}, \tag{18}$$

$$A_4 = \left[(1-\phi_2)\phi_1\frac{(\rho c_p)_{s_1}}{(\rho c_p)_{bf}} + \phi_2\frac{(\rho c_p)_{s_2}}{(\rho c_p)_{bf}} + (1-\phi+\phi_1\phi_2)\right].$$

where subscripts bf, nf, hnf, s_1, s_2 represent base fluid, nanofluid, hybrid nanofluid, alumina nanoparticles, and copper nanoparticles, respectively.

At the stretched sheet, the shear stress, $\tau_w(x)$ and the heat flux, $q_w(x)$ are the most essential heat transfer as well as flow parameters, and can be specified as [3]

$$\tau_w(x) = \mu_{hnf}\left(\frac{\partial u}{\partial y}\right)_{y=0}, \tag{19}$$

$$q_w(x) = -k_{hnf}\left(\frac{\partial T}{\partial y}\right)_{y=0} \tag{20}$$

Using Eq. (19) to (20) and similarity Eq. (6) to (8), the dimensionless local skin friction and heat transfer coefficients are [3]

$$C_f Re^{\frac{1}{2}} = \frac{1}{\xi}\left[\frac{1}{(1-\phi_1)^{2.5} + (1-\phi_2)^{2.5}}\right]f''(0), \tag{21}$$

$$Nu_x Re^{-\frac{1}{2}} = -\frac{1}{\xi}\left(\frac{k_{hnf}}{k_f}\right)\theta'(0), \tag{22}$$

where $Re = \frac{xu_w}{v_f}$ is the Reynold number [22].

3. Methodology

The HAM is proposed to find the thin-film thickness, λ by using MATHEMATICA software since λ is an unknown constant with continuous function between the range of $\eta = [0,1]$ and should be determined before the computational process [29]. HAM was first proposed by Shi-Jun Liao [49]. The method has been applied in previous studies by Faizan *et al.,* [50]. The approach provides an efficient procedure for explicitly and numerically solving a broad and generic class of differential systems that represent real-world physical issues. Figure 2 displays the HAM's steps.
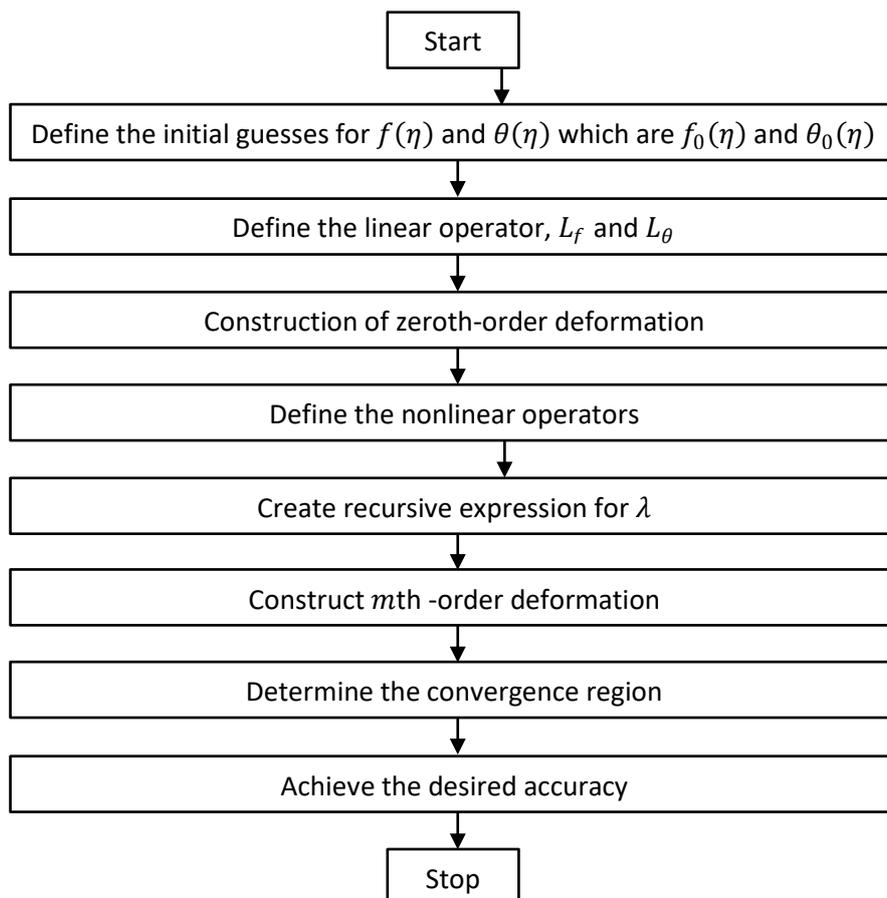
Fig. 2. Procedure for finding λ using HAM

The heat transfer mechanisms of the liquid film were then solved in MATLAB software utilizing the unconditionally stable implicit difference methodology known as the Keller box method for the iterated computational program and graph plotting. The approach is described in depth by Cebeci and Bradshaw [51]'s book. This method consists of four main steps as follows

    i.   simplify the governing equations to form a first-order system by introducing the new dependent variables $f = f, f' = u, f'' = v, \theta = \theta, \theta' = g$. Hence, yield

$$\left(\frac{A_1}{A_2}\right)\left(1 + \frac{1}{\beta}\right)v' + \lambda\left[fv - u^2 - S\left(u + \frac{1}{2}\eta v\right)\right] = 0, \tag{26}$$

$$\left(\frac{A_3}{A_4}\right)Pr^{-1}g' + \lambda\left(fg - 2\theta u - \frac{1}{2}S\eta g - \frac{3}{2}S\theta\right) = 0, \tag{27}$$

and the boundary conditions become

$$\begin{aligned}
\eta = 0: \ & f = 0, u = 1, \theta = 1, \\
\eta = 1: \ & f = \frac{S}{2}, v = 0, g = 0.
\end{aligned} \tag{28}$$

ii. using the central differences approach, the first-order system is expressed in a finite difference scheme. Generally, the derivatives in the $\eta -$directions and any points are defined as

$$p' = \frac{\partial p}{\partial \eta} = \frac{p_j - p_{j-1}}{h_j}, \text{ and } p_j = \frac{1}{2}(p_j - p_{j-1}). \tag{29}$$

iii. use the Newton approach to linearize the nonlinear equation. For example

$$f_j^{(i+1)} = f_j^{(i)} + \delta f_j^{(i)}. \tag{30}$$

i. compute the linear system using the block-elimination approach in form of a matrix. The matrix is written in the form of

$$[A][\delta] = [r]. \tag{31}$$

where matrix A is zero excluding those three along the diagonal. Then, the vector matrix can be written as

$$\begin{bmatrix} [A_1] & [C_1] & & & & \\ [B_2] & [A_2] & [C_2] & & & \\ & & \ddots & & & \\ & & & \ddots & & \\ & & & \ddots & & \\ & & & [B_{j-2}] & [A_{j-2}] & [C_{j-2}] \\ & & & & [B_J] & [A_J] \end{bmatrix} \begin{bmatrix} [\delta_1] \\ [\delta_2] \\ \vdots \\ \vdots \\ \vdots \\ [\delta_{j-1}] \\ [\delta_J] \end{bmatrix} = \begin{bmatrix} [r_1] \\ [r_2] \\ \vdots \\ \vdots \\ \vdots \\ [r_{j-1}] \\ [r_J] \end{bmatrix}, \tag{32}$$

4. Results and Discussion

The outcomes of the calculation resolution of the leading Eq. (13) to (16) are provided in tabular and graphical representations in sets of normalized local heat transfer rate and reduced skin friction. The current approach is confirmed by comparing the acquired numerical results to those obtained by Wang [29]. It is noticed that the current results are discovered to be in amazing concurrence with the distributed results as shown in Table 2 for the value of λ when $S = 0.8$ by using the HAM-based algorithm BVPh2.0. In addition, Table 3 also compares the numerical results of the Keller box approach to the earlier publication. It has been observed that the current findings are in astounding agreement with the dispersed outcomes.

In the mass transition situation, Figure 3 and 4 indicate the influence of the Casson parameter, β on the velocity and temperature distributions. Referring to these figures is comprehended that the λ is a decreasing function of the β. The thin-film at the free surface turns thinner. However, the growth of the β drops off the momentum boundary layer thickness of the thin-film. From the definition of the Casson parameter, an increase in the values of β gives the lessening in the yield stress that acts on the fluid and at the same time corresponds to enhance the plastic dynamic viscosity. In this case, the fluid behaves like a Newtonian fluid. Boosting the plastic viscosity that induces resistance in the motion of the fluid molecules, which is capable of reducing the velocity in the film fluid. On the other hand, enrichment in the β prompts to uplift the temperature distribution thus causing their

associated thermal boundary layer thickness to intensify. It is evident that the thinner of the thin-film aids the Casson fluid to gain more heat to beat the cohesive and adhesive attraction of the thin-film particles under mass transition effect. Figure 5 and 6 portray the fluctuation of velocity and temperature distributions for different value of ϕ_2. As the concentrations of ϕ_2 are improved in the hybrid nanofluid film, the λ reduces. The decrementation of the λ leads to the decay of the liquid film. Furthermore, the increase of the ϕ_2 leads to a decline in the velocity distribution. Physically, this could be due to the fact that any increase in the concentration of ϕ_2 results in boosting the viscosity of the fluid which prevents the molecules from moving smoothly in the thin-film. Hence, the momentum boundary layer thins and approaches zero of the thin-film thickness, $\eta = 0$.

When the liquid film with hybrid nanoparticles is closer to the elastic sheet, it inhibits the elastic from stretching due to the viscosity of the hybrid nanoparticles. However, the thermal boundary layer demonstrates opposite trends. The incrementation of the nanoparticles ϕ_2 upsurges the thermal conductivity in the fluid, thereby increasing the amount of heat in the thin-film flow. The nanoparticles disperse energy in the form of warmth. When the fluid is concentrated with the nanoparticles ϕ_2 the more heat will be utilized along with thinner thin-film thickness, producing a rise in temperature and thermal boundary layer thickness. The effect of injection parameter, w on the dimensionless velocity and temperature distributions are revealed in Figure 7 and 8, respectively. The movement of the fluid becomes slower in the film when the value of w is increased which in turn affects the boundary layer. The decelerated fluid velocity slows down the motion of the molecules in the fluid regime and thereby curtailing the momentum boundary layer. Notably that the temperature distribution clarifies the look-alike as a velocity distribution which is disclosed in Figure 8 when the stretching sheet is associated with the injection parameter.

Table 2
Comparison of ξ and $f''(0)$ for varying parameters of S by using HAM

S	$\xi\left(\lambda^{\frac{1}{2}}\right)$		$f''(0)$	
	Wang [29]	Present study	Wang [29]	Present study
0.7	2.57701	2.57692	-3.14965	-3.14954
0.8	2.15199	2.15199	-2.68094	-2.68363
0.9	1.81599	1.81599	-2.29683	-2.29683
1.0	1.54362	1.54362	-1.97238	-1.97238

Table 3
Comparison of $\theta(1)$ and $-\theta'(\eta)$ for $\phi_1 = \phi_2 = w = 0$ and $S = 0.8$ for various values of Pr

Pr	$\theta(1)$		$-\theta'(\eta)$	
	Wang [29]	Present study	Wang [29]	Present study
0.01	0.9605	0.9605	0.0905	0.0905
0.1	0.6925	0.6925	0.7562	0.7562
1.0	0.0979	0.0981	3.5960	3.5918
2.0	0.0249	0.0249	5.2442	5.2501
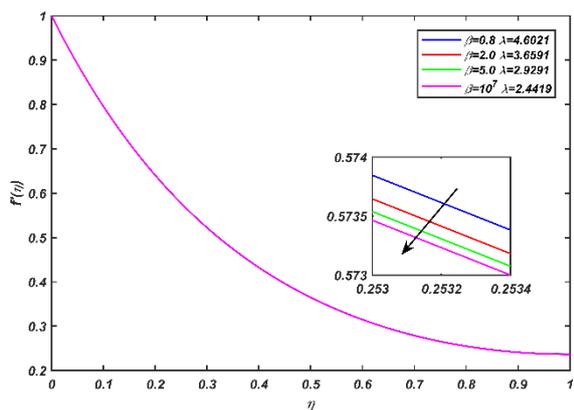
Fig. 3. $f'(\eta)$ for β
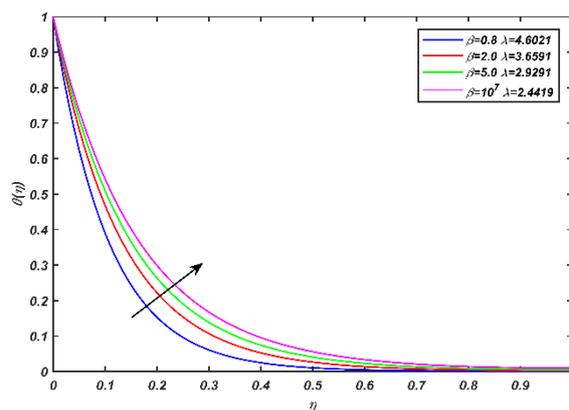
Fig. 4. $\theta(\eta)$ for β
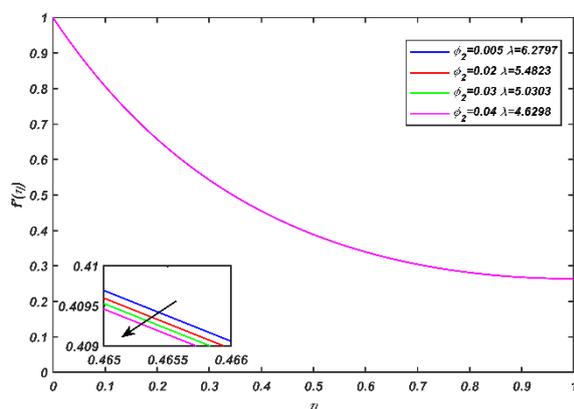
Fig. 5. $f'(\eta)$ for ϕ_2
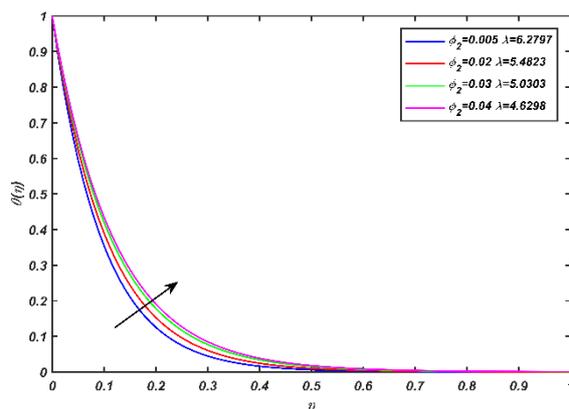
Fig. 6. $\theta(\eta)$ for ϕ_2
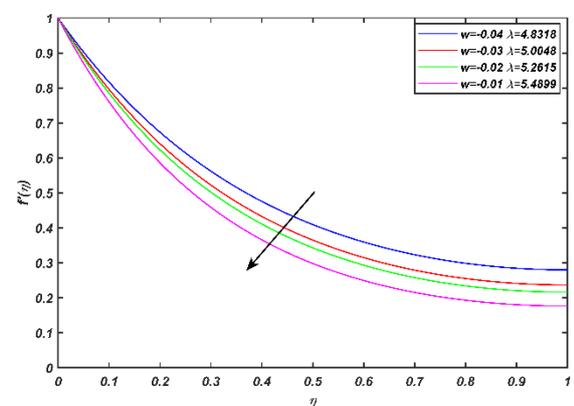
Fig. 7. $f'(\eta)$ for w
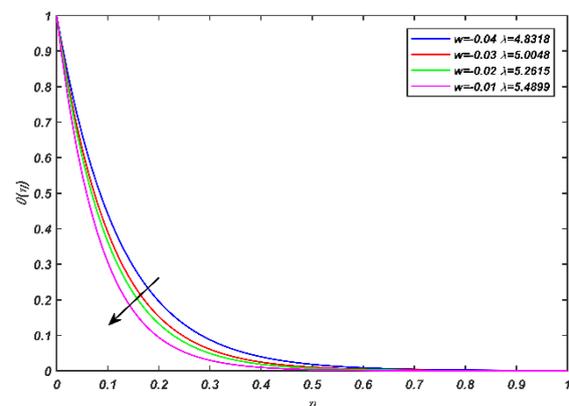
Fig. 8. $\theta(\eta)$ for w

Table 4 illustrates the local skin friction, $C_f Re_x^{\frac{1}{2}}$ and Nusselt number, $Nu_x Re_x^{-\frac{1}{2}}$ for various values of the pertinent parameters. Increasing the rate of the Casson parameter, β reduces the $C_f Re_x^{\frac{1}{2}}$ together with the λ, thereby lessening the wall shear stress at the surface of the stretching sheet. $Nu_x Re_x^{-\frac{1}{2}}$ has a similar performance under the mass transition effect that causes the temperature of the hybrid nanofluid to rise in a thinner layer. Further, $C_f Re_x^{\frac{1}{2}}$ declined immensely when the values of the concentration of nanoparticles volume fraction were enhanced. Thus, it minimizes the shear

stress on the sheet's wall during stretching. The results show that $Nu_x Re_x^{-\frac{1}{2}}$ depreciates the functions of β, ϕ_2 and w. Therefore, the decrement of the λ at the free surface was detected.

Table 4

Local skin friction, $C_f Re_x^{\frac{1}{2}}$ and Nusselt number, $Nu_x Re_x^{-\frac{1}{2}}$ on the various values of β, ϕ_2 and w

β	ϕ_2	w	$C_f Re_x^{\frac{1}{2}}$	$Nu_x Re_x^{-\frac{1}{2}}$
0.8			-2.3349	9.3774
2.0			-2.3363	7.6171
5.0			-2.3371	6.7899
10^7			-2.3376	6.1719
	0.005		-2.3343	10.2925
	0.020		-2.3349	9.3774
	0.030		-2.3357	8.3320
	0.040		-2.3362	7.4265
		-0.04	-1.9872	7.5665
		-0.03	-2.0721	8.1447
		-0.02	-2.1543	8.7620
		-0.01	-2.3349	9.3774

5. Conclusions

This report concentrated on the numerical analysis of an unsteady thin-film Casson hybrid nanofluid's heat transfer, boundary layer flow, and stretching sheet under the impact of mass transition. The assumed hybrid nanofluid model namely Tiwari and Das's model comprises alumina and copper as nanoparticles and ethylene glycol plus water as a base fluid. The problem is addressed numerically. Some observations from this study are as follows

  i.   Thin-film thickness declines for mass transition with the increment in Casson and nanoparticles volume fraction.
  ii. In mass transition conditions, enhancement in Casson and nanoparticles volume fraction declines the velocity distribution.
  iii. In mass transition settings, the fluid temperature increases as a function of Casson and the nanoparticle's volume fraction.
  iv. An increase in Casson and nanoparticles volume fraction diminished the local skin friction but Nusselt numbers are noted to be reduced.
  v.   Thin-film thickness, velocity distribution, temperature distribution, and local skin friction are seen to decrease as fluid flow mass transition increases, although the Nusselt number increases.

References

[1] Choi, S. US, and Jeffrey A. Eastman. *Enhancing thermal conductivity of fluids with nanoparticles*. No. ANL/MSD/CP-84938; CONF-951135-29. Argonne National Lab.(ANL), Argonne, IL (United States), 1995.

[2] Khan, W. A., and I. Pop. "Boundary-layer flow of a nanofluid past a stretching sheet." *International journal of heat and mass transfer* 53, no. 11-12 (2010): 2477-2483. https://doi.org/10.1016/j.ijheatmasstransfer.2010.01.032

[3] Jahan, Shah, Hamzah Sakidin, Roslinda Nazar, and Ioan Pop. "Unsteady flow and heat transfer past a permeable stretching/shrinking sheet in a nanofluid: A revised model with stability and regression analyses." *Journal of Molecular Liquids* 261 (2018): 550-564. https://doi.org/10.1016/j.molliq.2018.04.041

[4] Tiwari, Raj Kamal, and Manab Kumar Das. "Heat transfer augmentation in a two-sided lid-driven differentially heated square cavity utilizing nanofluids." *International Journal of heat and Mass transfer* 50, no. 9-10 (2007): 2002-2018. https://doi.org/10.1016/j.ijheatmasstransfer.2006.09.034

[5] Yirga, Y., and B. Shankar. "MHD flow and heat transfer of nanofluids through a porous media due to a stretching sheet with viscous dissipation and chemical reaction effects." *International Journal for Computational Methods in Engineering Science and Mechanics* 16, no. 5 (2015): 275-284. https://doi.org/10.1080/15502287.2015.1048385

[6] Hafidzuddin, Mohd Ezad Hafidz, Kohilavani Naganthran, Roslindar Nazar, and Norihan Md Arifin. "Effect of suction on the MHD fluid flow past a non-linearly stretching/shrinking sheet: Dual solutions." In *Journal of Physics: Conference Series*, vol. 1366, no. 1, p. 012027. IOP Publishing, 2019. https://doi.org/10.1088/1742-6596/1366/1/012027

[7] Gangadhar, K., T. Kannan, K. DasaradhaRamaiah, and G. Sakthivel. "Boundary layer flow of nanofluids to analyse the heat absorption/generation over a stretching sheet with variable suction/injection in the presence of viscous dissipation." *International Journal of Ambient Energy* 41, no. 9 (2020): 969-980. https://doi.org/10.1080/01430750.2018.1501738

[8] Jamshed, Wasim, Marjan Goodarzi, M. Prakash, Kottakkaran Sooppy Nisar, M. Zakarya, and Abdel-Haleem Abdel-Aty. "Evaluating the unsteady Casson nanofluid over a stretching sheet with solar thermal radiation: An optimal case study." *Case Studies in Thermal Engineering* 26 (2021): 101160. https://doi.org/10.1016/j.csite.2021.101160

[9] Nandeppanavar, Mahantesh M., S. Vaishali, M. C. Kemparaju, and N. Raveendra. "Theoretical analysis of thermal characteristics of casson nano fluid flow past an exponential stretching sheet in Darcy porous media." *Case Studies in Thermal Engineering* 21 (2020): 100717. https://doi.org/10.1016/j.csite.2020.100717

[10] Tawade, Jagadish V., C. N. Guled, Samad Noeiaghdam, Unai Fernandez-Gamiz, Vediyappan Govindan, and Sundarappan Balamuralitharan. "Effects of thermophoresis and Brownian motion for thermal and chemically reacting Casson nanofluid flow over a linearly stretching sheet." *Results in Engineering* 15 (2022): 100448. https://doi.org/10.1016/j.rineng.2022.100448

[11] Rawi, Noraihan Afiqah, Mohd Rijal Ilias, Lim Yeou Jiann, Zaiton Mat Isa, and Sharidan Shafie. "The effect of copper nanoparticles on mixed convection flow of jeffrey fluid induced by g-jitter." *Journal of Nanofluids* 7, no. 1 (2018): 156-162. https://doi.org/10.1166/jon.2018.1433

[12] Alkasasbeh, Hamzeh, Mohammed Swalmeh, Hebah Bani Saeed, Feras Al Faqih, and Adeeb Talafha. "Investigation on CNTs-water and human blood based Casson nanofluid flow over a stretching sheet under impact of magnetic field." *Frontiers in Heat and Mass Transfer (FHMT)* 14 (2020). https://doi.org/10.5098/hmt.14.15

[13] Casson, N. "Flow equation for pigment-oil suspensions of the printing ink-type." *Rheology of disperse systems* (1959): 84-104.

[14] Hussanan, Abid, Mohd Zuki Salleh, Ilyas Khan, and Sharidan Shafie. "Analytical solution for suction and injection flow of a viscoplastic Casson fluid past a stretching surface in the presence of viscous dissipation." *Neural computing and applications* 29 (2018): 1507-1515. https://doi.org/10.1007/s00521-016-2674-0

[15] Vinogradov, Georgii Vladimirovich, and A. Ya Malkin. *Rheology of polymers: viscoelasticity and flow of polymers*. Moscow: Mir, 1980. https://doi.org/10.1007/978-3-642-52204-8

[16] Ali, Hafiz Muhammad, ed. *Hybrid nanofluids for convection heat transfer*. Academic Press, 2020.

[17] Devi, SP Anjali, and S. Suriya Uma Devi. "Numerical investigation of hydromagnetic hybrid Cu–Al2O3/water nanofluid flow over a permeable stretching sheet with suction." *International Journal of Nonlinear Sciences and Numerical Simulation* 17, no. 5 (2016): 249-257. https://doi.org/10.1515/ijnsns-2016-0037

[18] Waini, Iskandar, Anuar Ishak, and Ioan Pop. "Unsteady flow and heat transfer past a stretching/shrinking sheet in a hybrid nanofluid." *International journal of heat and mass transfer* 136 (2019): 288-297. https://doi.org/10.1016/j.ijheatmasstransfer.2019.02.101

[19] Maleki, Hamid, Mohammad Reza Safaei, Hussein Togun, and Mahidzal Dahari. "Heat transfer and fluid flow of pseudo-plastic nanofluid over a moving permeable plate with viscous dissipation and heat absorption/generation." *Journal of Thermal Analysis and Calorimetry* 135 (2019): 1643-1654. https://doi.org/10.1007/s10973-018-7559-2

[20] Venkateswarlu, Bhumavarapu, and Panyam Venkata Satya Narayana. "Cu-Al2O3/H2O hybrid nanofluid flow past a porous stretching sheet due to temperatue-dependent viscosity and viscous dissipation." *Heat Transfer* 50, no. 1 (2021): 432-449. https://doi.org/10.1002/htj.21884

[21] Sakkaravarthi, K., and P. Bala Anki Reddy. "Entropy generation on Casson hybrid nanofluid over a curved stretching sheet with convective boundary condition: Semi-analytical and numerical simulations." *Proceedings of the Institution of Mechanical Engineers, Part C: Journal of Mechanical Engineering Science* 237, no. 2 (2023): 465-481. https://doi.org/10.1177/09544062221119055

[22] Sulochana, C., and S. R. Aparna. "Unsteady magnetohydrodynamic radiative liquid thin film flow of hybrid nanofluid with thermophoresis and Brownian motion." *Multidiscipline Modeling in Materials and Structures* (2019). https://doi.org/10.1108/MMMS-08-2019-0160

[23] Girtan, Mihaela, and Mihaela Girtan. "New trends in solar cells research." *Future Solar Energy Devices* (2018): 45-75. https://doi.org/10.1007/978-3-319-67337-0_3

[24] Wang, C. Y. "Liquid film on an unsteady stretching surface." *Quarterly of applied Mathematics* 48, no. 4 (1990): 601-610. https://doi.org/10.1090/qam/1079908

[25] Sakiadis, B. C. "Boundary-layer behavior on continuous solid surfaces: II. The boundary layer on a continuous flat surface." *AIChE journal* 7, no. 2 (1961): 221-225. https://doi.org/10.1002/aic.690070211

[26] Crane, Lawrence J. "Flow past a stretching plate." *Zeitschrift für angewandte Mathematik und Physik ZAMP* 21 (1970): 645-647. https://doi.org/10.1007/BF01587695

[27] Carragher, P., and L. J. Crane. "Heat transfer on a continuous stretching sheet." *Zeitschrift Angewandte Mathematik und Mechanik* 62, no. 10 (1982): 564-565. https://doi.org/10.1515/9783112546901-009

[28] Andersson, Helge I., Jan B. Aarseth, and Bhabani S. Dandapat. "Heat transfer in a liquid film on an unsteady stretching surface." *International Journal of Heat and Mass Transfer* 43, no. 1 (2000): 69-74. https://doi.org/10.1016/S0017-9310(99)00123-4

[29] Wang, Chun. "Analytic solutions for a liquid film on an unsteady stretching surface." *Heat and Mass Transfer* 42 (2006): 759-766. https://doi.org/10.1007/s00231-005-0027-0

[30] Xu, Hang, Ioan Pop, and Xiang-Cheng You. "Flow and heat transfer in a nano-liquid film over an unsteady stretching surface." *International Journal of Heat and Mass Transfer* 60 (2013): 646-652. https://doi.org/10.1016/j.ijheatmasstransfer.2013.01.046

[31] Giri, Shib Sankar, Kalidas Das, and Prabir Kumar Kundu. "Inclined magnetic field effects on unsteady nanofluid flow and heat transfer in a finite thin film with non-uniform heat source/sink." *Multidiscipline Modeling in Materials and Structures* 15, no. 1 (2019): 265-282. https://doi.org/10.1108/MMMS-04-2018-0065

[32] Turkyilmazoglu, Mustafa. "Nanoliquid film flow due to a moving substrate and heat transfer." *The European Physical Journal Plus* 135 (2020): 1-13. https://doi.org/10.1140/epjp/s13360-020-00812-y

[33] Pal, Dulal, Debranjan Chatterjee, and Surya Kanta Mondal. "Heat and mass transfer in thin nanoliquid film over an unsteady stretching sheet in a porous medium with chemical reaction and thermal radiation." *International Journal of Ambient Energy* 43, no. 1 (2022): 845-852. https://doi.org/10.1080/01430750.2019.1676308

[34] Lu, Dianchen, Muhammad Ramzan, Mutaz Mohammad, Fares Howari, and Jae Dong Chung. "A thin film flow of nanofluid comprising carbon nanotubes influenced by Cattaneo-Christov heat flux and entropy generation." *Coatings* 9, no. 5 (2019): 296. https://doi.org/10.3390/coatings9050296

[35] Ohring, Milton. "Material Science of Thin Films. Stevens Institute of Technology." (2001).

[36] Rehman, Sajid, M. Idrees, Rehan Ali Shah, and Zeeshan Khan. "Suction/injection effects on an unsteady MHD Casson thin film flow with slip and uniform thickness over a stretching sheet along variable flow properties." *Boundary Value Problems* 2019, no. 1 (2019): 1-24. https://doi.org/10.1186/s13661-019-1133-0

[37] Tawade, Jagadish V., Mahadev Biradar, and Shaila S. Benal. "Influence of Radiant Heat and Non-uniform Heat Source on MHD Casson Fluid Flow of Thin Liquid Film Beyond a Stretching Sheet." In *Recent Trends in Mathematical Modeling and High Performance Computing: M3HPCST-2020, Ghaziabad, India, January 9-11, 2020*, pp. 23-36. Springer International Publishing, 2021. https://doi.org/10.1007/978-3-030-68281-1_3

[38] Ray, Atul Kumar, B. Vasu, O. Anwar Bég, Rama Subba Reddy Gorla, and P. V. S. N. Murthy. "Magneto-bioconvection flow of a Casson thin film with nanoparticles over an unsteady stretching sheet: HAM and GDQ computation." *International Journal of Numerical Methods for Heat & Fluid Flow* 29, no. 11 (2019): 4277-4309. https://doi.org/10.1108/HFF-02-2019-0158

[39] Alali, Elham, and Ahmed M. Megahed. "MHD dissipative Casson nanofluid liquid film flow due to an unsteady stretching sheet with radiation influence and slip velocity phenomenon." *Nanotechnology Reviews* 11, no. 1 (2022): 463-472. https://doi.org/10.1515/ntrev-2022-0031

[40] Sandhya, G., K. Malleswari, G. Sarojamma, K. Sreelakshmi, and PV Satya Narayana. "Unsteady Casson nanofluid thin film flow over a stretching sheet with viscous dissipation and chemical reaction." *The European Physical Journal Special Topics* 230 (2021): 1381-1390. https://doi.org/10.1140/epjs/s11734-021-00033-z

[41] Alhussain, Ziyad A., and Asifa Tassaddiq. "Thin film blood based Casson hybrid nanofluid flow with variable viscosity." *Arabian Journal for Science and Engineering* 47, no. 1 (2022): 1087-1094. https://doi.org/10.1007/s13369-021-06067-8

[42] Bi, Sheng-shan, Lin Shi, and Li-li Zhang. "Application of nanoparticles in domestic refrigerators." *Applied Thermal Engineering* 28, no. 14-15 (2008): 1834-1843. https://doi.org/10.1016/j.applthermaleng.2007.11.018

[43] Bi, Sheng-shan, Lin Shi, and Li-li Zhang. "Application of nanoparticles in domestic refrigerators." *Applied Thermal Engineering* 28, no. 14-15 (2008): 1834-1843. https://doi.org/10.1016/j.applthermaleng.2007.11.018

[44] Aziz, Raziana Che, Ishak Hashim, and A. K. Alomari. "Flow and heat transfer in a liquid film over a permeable stretching sheet." *Journal of Applied Mathematics* 2013 (2013). https://doi.org/10.1155/2013/487586

[45] Ali, Farhan, T. Arun Kumar, K. Loganathan, C. S. Reddy, Amjad Ali Pasha, Mustafa Mutiur Rahman, and Khaled Al-Farhany. "Irreversibility analysis of cross fluid past a stretchable vertical sheet with mixture of Carboxymethyl cellulose water based hybrid nanofluid." *Alexandria Engineering Journal* 64 (2023): 107-118. https://doi.org/10.1016/j.aej.2022.08.037

[46] Ali, F., K. Loganathan, S. Eswaramoorthi, K. Prabu, A. Zaib, and Dinesh Kumar Chaudhary. "Heat transfer analysis on carboxymethyl cellulose water-based cross hybrid nanofluid flow with entropy generation." *Journal of Nanomaterials* 2022 (2022). https://doi.org/10.1155/2022/5252918

[47] Lin, Yanhai, Liancun Zheng, and Goong Chen. "Unsteady flow and heat transfer of pseudo-plastic nanoliquid in a finite thin film on a stretching surface with variable thermal conductivity and viscous dissipation." *Powder Technology* 274 (2015): 324-332. https://doi.org/10.1016/j.powtec.2015.01.039

[48] Teh, Yuan Ying, and Adnan Ashgar. "Three dimensional MHD hybrid nanofluid Flow with rotating stretching/shrinking sheet and Joule heating." *CFD Letters* 13, no. 8 (2021): 1-19. https://doi.org/10.37934/cfdl.13.8.119

[49] Liao, Shijun. *Beyond perturbation: introduction to the homotopy analysis method*. CRC press, 2003.

[50] Faizan, Muhammad, Farhan Ali, Karuppusamy Loganathan, Aurang Zaib, Ch Achi Reddy, and Sara I. Abdelsalam. "Entropy Analysis of Sutterby Nanofluid Flow over a Riga Sheet with Gyrotactic Microorganisms and Cattaneo–Christov Double Diffusion." *Mathematics* 10, no. 17 (2022): 3157. https://doi.org/10.3390/math10173157

[51] Cebeci, Tuncer, and Peter Bradshaw. *Physical and computational aspects of convective heat transfer*. Springer Science & Business Media, 2012.